

Dark Matter in Galaxies: evidences and challenges

Paolo Salucci

Received: date / Accepted: date

Abstract The evidence of the phenomenon for which, in galaxies, the gravitating mass is distributed differently than the luminous mass, increases as new data become available. Furthermore, this discrepancy is well structured and it depends on the magnitude and the compactness of the galaxy and on the radius, in units of its luminous size R_{opt} , where the measure is performed. For the disk systems with $-13 \geq M_I \geq -24$ all this leads to an amazing scenario, revealed by the investigation of individual and coadded rotation curves, according to which, the circular velocity follows, from their centers out to their virial radii, an universal profile $V_{URC}(r/R_{opt}, M_I)$ function only of the properties of the luminous mass component. Moreover, from the Universal Rotation Curve, so as from many individual high quality RCs, we discover that, in the innermost regions of galaxies, the DM halo density profiles are very shallow. Finally, the disk mass, the central halo density and its core radius, come out all related to each other and to two properties of the distribution of light in galaxies: the luminosity and the compactness. This phenomenology, being absent in the simplest Λ CDM Cosmology scenario, poses serious challenges to the latter or, alternatively, it requires a substantial and tuned involvement of baryons in the formation of the galactic halos. On the other side, the URC helps to explain the two-accelerations relationship found by McGaugh et al 2016, in terms of only well known astrophysical processes, acting in a standard DM halos + luminous disks scenario.

Keywords Dark Matter · Galaxies

1 Introduction

The presence of huge content of invisible matter in and around spiral galaxies, distributed differently from stars and gas, is well determined from optical and 21

P Salucci
SISSA
Tel.: +39-40-3787520
Fax: +39-40-3787528
E-mail: salucci@sissa.it

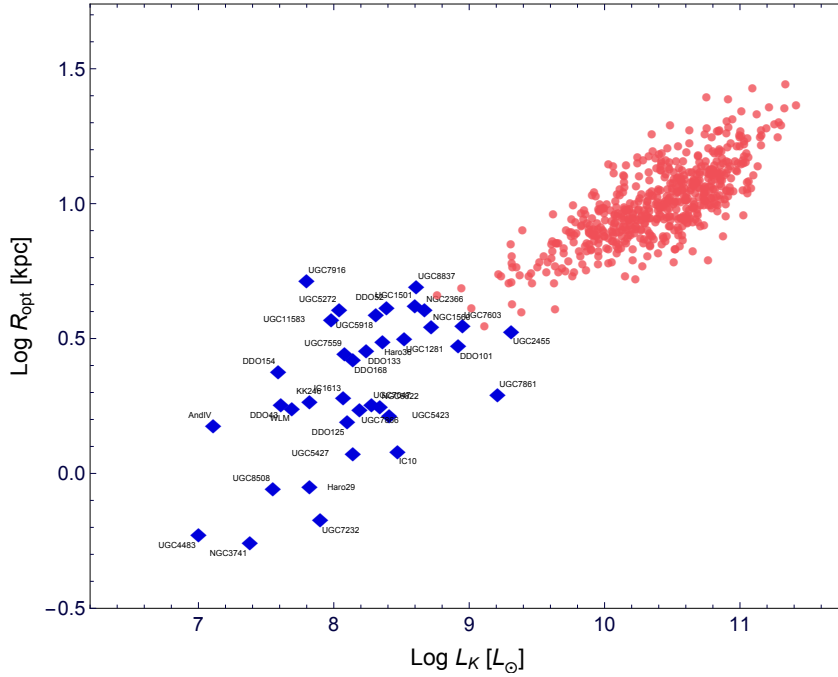


Fig. 1 The optical radius R_{opt} vs luminosity for spirals (red circles) and dwarf disks (blue diamonds)

cm rotation curves (RCs) [32, 2]. The extra mass component becomes progressively more abundant *i*) at outer radii and *ii*) at a same radius, in the less luminous galaxies ([30]). The total gravitational potential of spirals ϕ_{tot} includes different components: $\phi_{tot} = \phi_b + \phi_d + \phi_{HI} + \phi_{DM}$ namely, the bulge component, the stellar disk component, the HI disk component and finally the Dark Matter one. Φ_{tot} is related to the galaxy's circular velocity by:

$$V^2(r) = r \frac{d}{dr} \phi_{tot} = V_b^2 + V_d^2 + V_{HI}^2 + V_{DM}^2 \quad (1)$$

with all the R.H.S. terms function of radius r . The Poisson equation relates the surface/spatial densities to the corresponding gravitational potentials. Then, the velocity fields V_i are the solutions of the four separated Equations:

$$\nabla^2 \Phi_i = 4\pi G \rho_i \quad (2)$$

where the index i defines the 4 components of the total density: $\rho_b(r)$, $\mu_d(r)\delta(z)$, $\mu_{HI}(r)\delta(z)$, $\rho_{DM}(r)$, with $\delta(z)$ the Kronecker function and z the cylindrical coordinate. We can generally assume that the stellar surface density $\Sigma_d(r)$ is proportional to $\mu_d(r)$, well measured by CCD infrared photometry, leading to the well-known Freeman exponential thin disk profile [14]

$$\Sigma_d(r) = \frac{M_D}{2\pi R_D^2} e^{-r/R_D}, \quad (3)$$

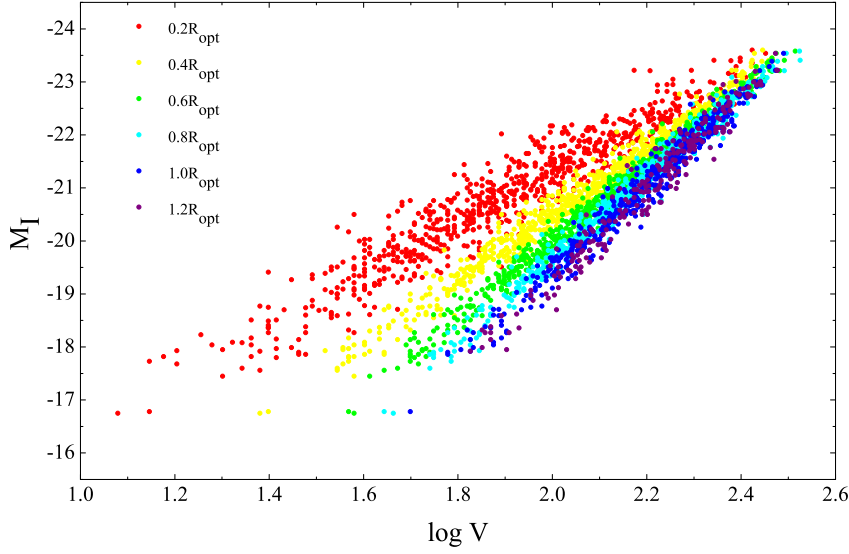


Fig. 2 The Radial Tully-Fisher: the ensemble of the relations at different radii measured in units of R_{opt} .

where M_D is the disk mass and R_D the scale length. $R_{opt} \equiv 3.2R_D$, the radius that encloses 83% of the total galaxy light, is usually adopted as the optical size of the galaxies. In Spirals, the two above quantities are well correlated (see Fig. (1) and [44]):

$$\log\left(\frac{R_D}{\text{kpc}}\right) = 0.633 + 0.379 \log\left(\frac{M_D}{10^{11}M_\odot}\right) + 0.069 \left(\log\frac{M_D}{10^{11}M_\odot}\right)^2, \quad (4)$$

From Eqs (2-3) and with $y \equiv r/R_D$ we have:

$$V_d^2(y) = \frac{GM_D}{2R_D} y^2 B\left(\frac{y}{2}\right) \quad (5)$$

where $y \equiv r/R_D$, G is the gravitational constant $B = I_0K_0 - I_1K_1$ a combination of Bessel functions evaluated at $1/2 y$, [14]. Let us stress that to adopt directly in Eq(2) the measured surface brightness, rather than its fitting function in Eq(3), changes no result of this work

The surface density of the HI disk $\Sigma_{HI}(r)$ is directly derived by 21 cm HI flux measurements and it can be approximately represented by $1/9 \Sigma_d(r/(3 R_D))(M_{HI}/M_D)$ [44], then:

$$V_{HI}^2(y) = \frac{M_{HI}}{9 M_D} V_d^2(y/3) \quad (6)$$

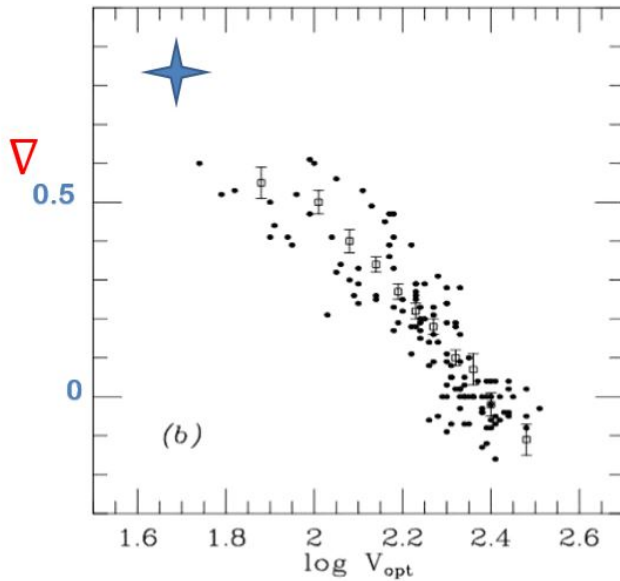


Fig. 3 The rotation curve slope $\nabla \equiv d \log V / d \log r$ at R_{opt} as a function of $\log V_{opt}$. The cross indicates the region of **dd** galaxies. Also shown the data from the 11 coadded (*open circles with errorbars*) and 131 individual (*filled circles*) RCs of [31].

Stellar Bulges are important contributors of the total galaxy mass only for early Hubble Types objects that are non-considered in this work.

Let us to introduce here, for any galaxy, the virial radius R_{vir} and the virial halo mass M_{vir} related by: $M_{vir} \simeq 100 \rho_c R_{vir}^3$ and ρ_c is the mean density of the Universe: $\rho_c = 1 \times 10^{-29} \text{ g/cm}^3$

The rotation curves of spirals show properties and an high degree of universality that cannot be explained by their baryonic matter content:

- **Amplitudes.** At any radius R_n , measured in units of R_{opt} such that: $R_n \equiv (n/5)R_{opt}$, ($n = 1, 7$), there is a tight relationship between the local rotation velocity $V_n \equiv V(R_n)$ and the total galaxy magnitude M_I [46]:

$$M_I = a_n \log V_n + b_n \quad (7)$$

The ensemble of relationships is shown in Fig (2); their r.m.s. scatter is always very small (< 0.3 magnitudes) and for $n = 3$ reaches a minimum of 0.12 magnitudes ([46]). This baffling result indicates that, in average, the I-magnitude is able to predict, in any galaxy and at any radius, the value of the circular velocity within a 5% uncertainty. Moreover, the evident increase of a_n with n , see Fig. (2) provides us with precious information on the mass distribution in Spirals [46].

- **Slopes** ∇ , the logarithmic slope of the circular velocity at R_{opt} emerges as a tight function of V_{opt} and of galaxy magnitude (see Fig(4) and also [31]). One finds: $-0.3 \leq \nabla \leq 1$ (see Fig. (3)). Let us also stress, that the quantity ∇ takes, in disk systems, all the values allowed in Newtonian Gravity, from -0.5 (Keplerian regime) to 1 (solid body regime), falsifying so, the paradigm of “flat rotation curves” according to which, in great prevalence, one should find: $\nabla = 0$.

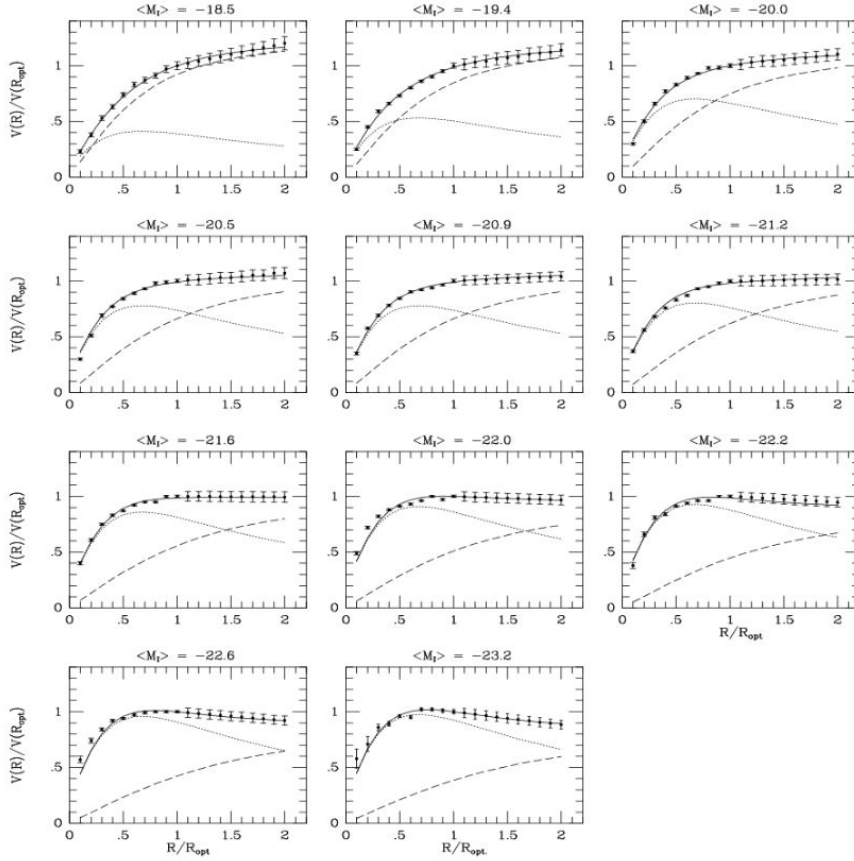


Fig. 4 The coadded RCs (*points*) and the Universal Rotation Curve of Spirals out to $6.4 R_D$ (*lines*). Also shown the dark (*dashed*) and the luminous (*pointed*) velocity components.

2 The Universal Rotation Curve of Spirals

We can represent the rotation curves of late types Spirals by means of the Universal Rotation Curve (URC) pioneered in [33,28] and set by [31] and [38]. The first step of the investigation of the spiral kinematics is the acquisition of 11 coadded rotation curves $V_{coadd}(r/R_{opt}, M_I)$ that are obtained, by binning and averaging in *a*) magnitude and *b*) normalized radius $x \equiv R/R_{opt}$, 967 extended and high quality rotation curves of late type spirals (published in [29]).

These 11 coadded RCs (*points* with errorbars in Fig(4)) extend out to $\simeq 2 R_{opt}$ and represent the full kinematics of spirals, whose I-magnitude range is $-16.3 < M_I < -23.4$. They lead to the Universal Rotation Curve (URC): i.e. a velocity model $V_{URC}(r/R_{opt}, M_I)$ function of radius and of luminosity, that well fits the $V_{coadd}(r/R_{opt}, M_I)$ data (see Fig(5) and [31,38]).

The URC is, therefore, a specific proper function of normalized radius, which, tuned by few parameters, namely the galaxy luminosity, well fits the coadded and

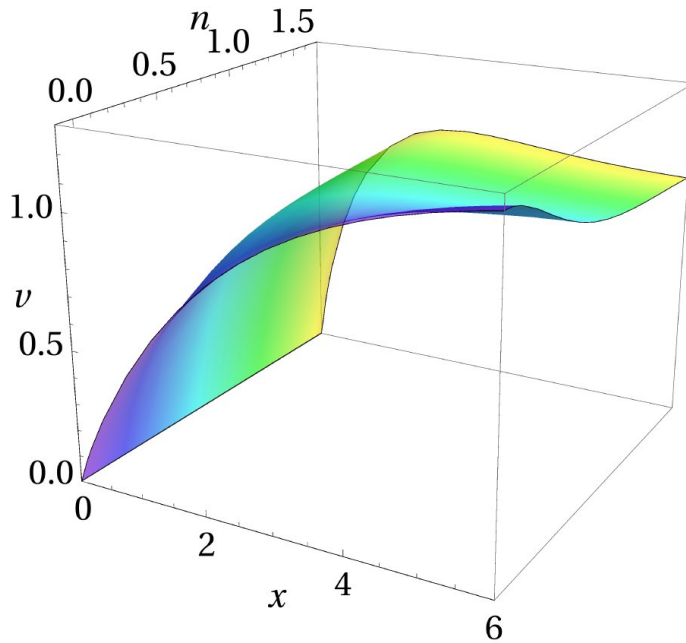


Fig. 5 The URC out to $2 R_{opt}$. We have: $n = \log M_{vir} - 11$, $v \equiv V(r/R_{opt})/V(R_{opt})$

individual rotation curves representing the RCs of more than 100k local spirals of different luminosity and Hubble type.

In detail, in the simplest version, the URC has two velocity components, one from the stellar disk and the other from the dark halo:

$$V_{URC}^2(x, M_I) = V_{URCd}^2(x, M_I) + V_{URCh}^2(x, M_I) \quad (8)$$

The first component is the standard Freeman disk of Eq. (4),

$$V_{URCd}^2(y) = \frac{GM_D}{2R_D} y^2 B\left(\frac{y}{2}\right) \quad (9)$$

The second is the Burkert halo velocity profile, proposed by [37] to represent the DM density in halos around galaxies of any magnitude or Hubble Type:

$$\rho(r) = \frac{\rho_0 r_0^3}{(r + r_0)(r^2 + r_0^2)}, \quad (10)$$

$$V_{URCh}^2(r) = 6.4 \frac{\rho_0 r_0^3}{r} \left(\ln\left(1 + \frac{r}{r_0}\right) - \arctan\left(\frac{r}{r_0}\right) + \frac{1}{2} \ln\left(1 + \frac{r^2}{r_0^2}\right) \right). \quad (11)$$

where ρ_0 and r_0 are, respectively, the DM central density and its core radius. The URC velocity model has then three parameters: M_D, ρ_0, r_0 that are obtained by best-fitting the 11 coadded rotation curves (that represent the kinematics of the whole family of normal Spirals). The fit is excellent (see Fig.(4) and [31]). The reduced $\chi^2 < 1$ and the uncertainties on the parameters are about 15%. Each

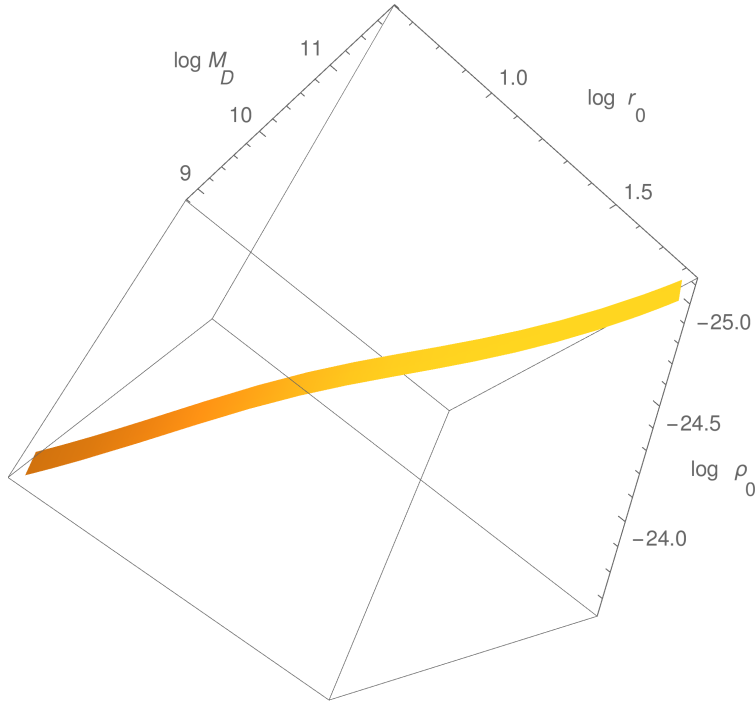


Fig. 6 The relationship among the URC parameters. Units: M_D in M_\odot , ρ_0 in g/cm^3 and r_0 in kpc.

parameter is related to all the others see Fig.(6) and they all are dependent on luminosity [38]. As far as the halo virial mass M_{vir} we have: ($M_s = 3 \times 10^{11} M_\odot$): $M_D = 2.3 \cdot 10^{10} (M_{vir}/M_s)^{3.1} / (1 + (M_{vir}/M_s)^{2.2})$

The mass distribution in Spirals as resulting from the URC (see [38] for details) has some specific characteristics. At any normalized radius x , objects with lower luminosity have a larger dark-to-stellar mass ratio. Moreover, spirals have a radius, whose size increases from $0.5R_D$ to $3R_D$ with galaxy luminosity, inside which the baryonic matter fully accounts for the rotation curve and outside which, a dark component is needed to justify the RC profile (see Fig (4)) in ([31]) Let us notice that the latter is the correct enunciation of the wellknown “maximum disk hypothesis.

Of particular importance is the quantity $\mu_{0D} \equiv \rho_0 r_0$, proportional to the halo central surface density, that results constant in objects of any magnitudes and Hubble Type, as pioneered by [20,9]:

$$\log \frac{\mu_{0D}}{M_\odot \text{pc}^{-2}} = 2.2 \pm 0.25 \quad (12)$$

This relationship is supported by independent work [42] and it can be considered as a portal leading to the nature itself of the dark matter [8] (see also Section 4).

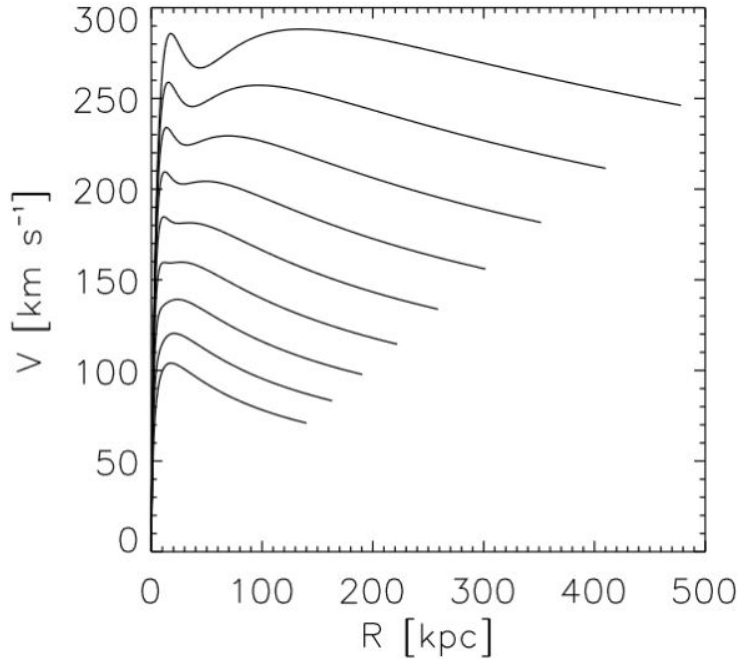


Fig. 7 The Universal Rotation Curve out to R_{vir} in physical units, see [38] for details

By means of a number of very extended RCs and of virial velocities $V_{vir} \equiv (GM_{vir}/R_{vir})^{1/2}$ obtained by means of the abundance matching method, [40], it is possible to determine with accuracy the halo mass [38] around a galaxy of magnitude M_I and therefore to extend the URC out to galaxie's virial radii (see Fig(7))

As result, in Spirals, the halo mass range is: $3 \times 10^{10} M_{\odot} \leq M_{vir} \leq 3 \times 10^{13} M_{\odot}$. The stellar to halo fraction M_D/M_{vir} ranges between 7×10^{-3} to 5×10^{-2} , [12], values much smaller than the cosmological one of $\Omega_b/\Omega_{matter} \simeq 1/6$,

3 Cuspy or Cored Dark Matter Halos in disk systems

The lack, in the DM halo density of Spirals, of the inner cuspieness predicted by N-Body simulations in (the simplest version of) the Λ Cold Dark Matter scenario[26] is a crucial evidence for the fields of Cosmology and in Astroparticle. In fact, in such scenario, the DM halo spatial density is universal and it is well reproduced by one-parameter radial profile [26]:

$$\rho_{NFW}(r) = \frac{\rho_s}{(r/r_s)(1+r/r_s)^2}, \quad (13)$$

where r_s is a characteristic inner radius, and ρ_s the corresponding density. It is clear that the NFW halo density diverges at the origin as r^{-1} . From Eq. (13) we get:

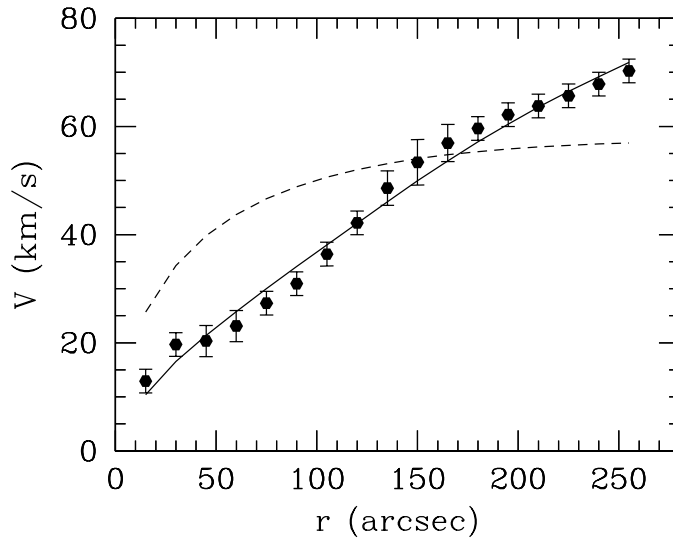


Fig. 8 Rotation curve of DDO 47 (*points*) vs models. Burkert halo + stellar/HI disks (*solid line*). NFW halo + stellar/HI disks (*dashed line*) (see [16])

$$V_{NFW}^2(r) = M_{vir} \frac{(\ln(1+r/r_s) - (r/r_s)/(1+r/r_s))}{\ln(1+c) - c/(1+c)} / r \quad (14)$$

with: $R_{vir}/r_s \simeq 9.7 \left(\frac{M_{vir}}{10^{12} M_{\odot}} \right)^{-0.13}$.

Since their emergence in numerical simulations, cuspy density profiles were claimed to disagree with the DM density profiles detected around dwarf spirals (e.g. [24]). However, strong concerns were raised on whether the evidence provided was biased by observational systematics.

A solution of the cusp-core controversy came from a careful modelling of 2D, high quality, extended rotation curves [15]. As result of this strategy, no cuspy behavior in the DM density has been found (e.g. [5,36]). Presently, none of the 100 most suitable and high quality RC can be satisfactorily reproduced by a NFW halo + stellar HI/disks velocity model. In virtually all the cases, instead, the cored model fits well the RC with reasonable values for the free parameters. As a test case, we consider the nearby dwarf spiral galaxy DDO 47 (see Fig.(8)). Its RC modelling finds that in this galaxy the dark halo density must have a core of ~ 7 kpc and a central density of $\rho_0 = 1.4 \times 10^{-24} \text{ g cm}^{-3}$. The NFW halo profile, instead, is totally unable to fit the RC see Fig (8).

It is important to stress that the cusped halo distributions do fail, not (only) because they fit poorly the RCs, but also because (see e.g. [15]):

- they often imply implausibly values for the stellar mass-to-light ratio and/or the halo mass

- they often do not follow the Λ CDM concentration vs halo mass relationship

Moreover, direct investigations of RCs have also ruled out the possibility that the detection of a cored distribution could be a mirage arisen by not-axisymmetric motions in the galaxy affecting the rotation curve (e.g. [16]).

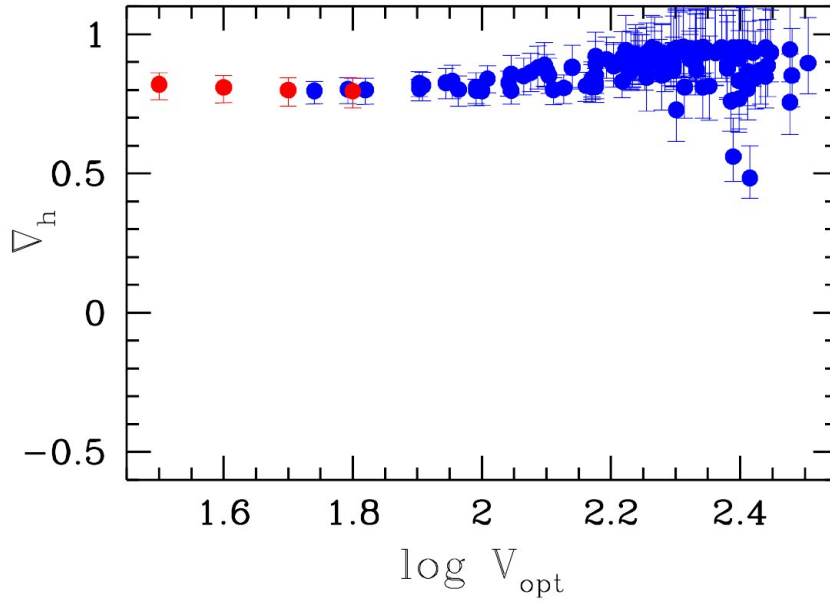


Fig. 9 ∇_h , the DM halo velocity slope at R_{opt} in Spirals (*blue*) and in **dd** (*red*). The NFW halo profiles have: $\nabla_{h,NFW} \simeq 0.2$

Finally, we notice that there are *model independent* evidences for cored DM halo density distributions. Salucci, (2001) [34] derived, for 140 spirals of different luminosity, ∇_h the logarithmic gradient of the halo contribution to the circular velocity at the edge of the stellar disk: $\nabla_h \equiv \frac{d \log V_h(r)}{d \log r}$ evaluated at R_{opt} (see Fig. (9)). He found: $\nabla_h \simeq 0.9$ in all galaxies, i.e. a value inconsistent with the predictions by the NFW density profile. For a large sample of Low Surface Brightness galaxies, a very similar result was obtained by [4].

4 The URC of dd galaxies

Karukes and Salucci, 2016 ([18]) selected a sample of 36 dwarf discs from the Local Volume Catalog, which is ~ 70 per cent complete down to $M_B \approx -14$ and out to 11 Mpc. The objects are bulgeless systems in which rotation, corrected for the pressure support, balances the gravitational force. Morphologically, they include gas-rich dwarfs star-forming at a relatively-low rate, and starbursting blue compact dwarfs (BCD). Hereafter, for simplicity, we call them dwarf disks (**dd**) that, for the DM investigation, is their principal characteristic. They have a Freeman surface luminosity profile but, differently from spirals, their L_K vs R_{opt} relationship has a very large scatter, see Fig.(1). The disc length scales R_D of the galaxies in the sample are known within 15 per cent uncertainty; their RCs are symmetric, smooth with small r.m.s. and extend out to $\sim 3 R_D$

In this sample that reaches 5 magnitudes down with respect to the least luminous spirals ([31]), the magnitudes, disc length scales and optical velocities

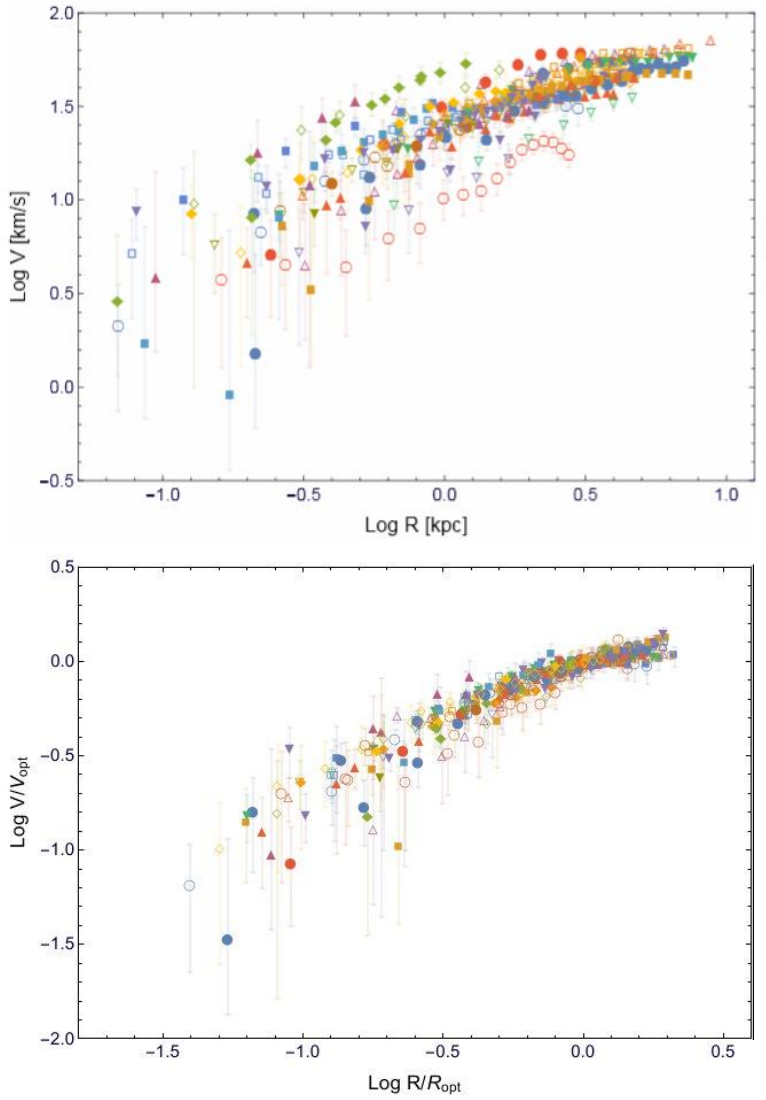


Fig. 10 Individual RCs of **dd**. In physical units (*top panel*). After the R_{opt} and V_{opt} double normalization (*bottom panel*). Each galaxy has its own color-shape code, see [18].

intervals are:

$$-19 < M_I < -13, \quad 0.18 \text{ kpc} < R_D < 1.63 \text{ kpc}, \quad 17 \text{ km/s} < V_{opt} < 61 \text{ km/s}$$

The average optical radius and optical velocity of the sample are: $\langle R_{opt} \rangle$ and $\langle V_{opt} \rangle$ are: 2.5 kpc , 40.0 km/s , respectively.

We plot, in the log-log scales, the 36 RCs of the **dd** sample expressed in physical units (Fig. 10 *top*). Contrary to the RCs of normal spirals [31], each **dd** rotation curve has a quite different shape, see also [27]. Although all curves increase with

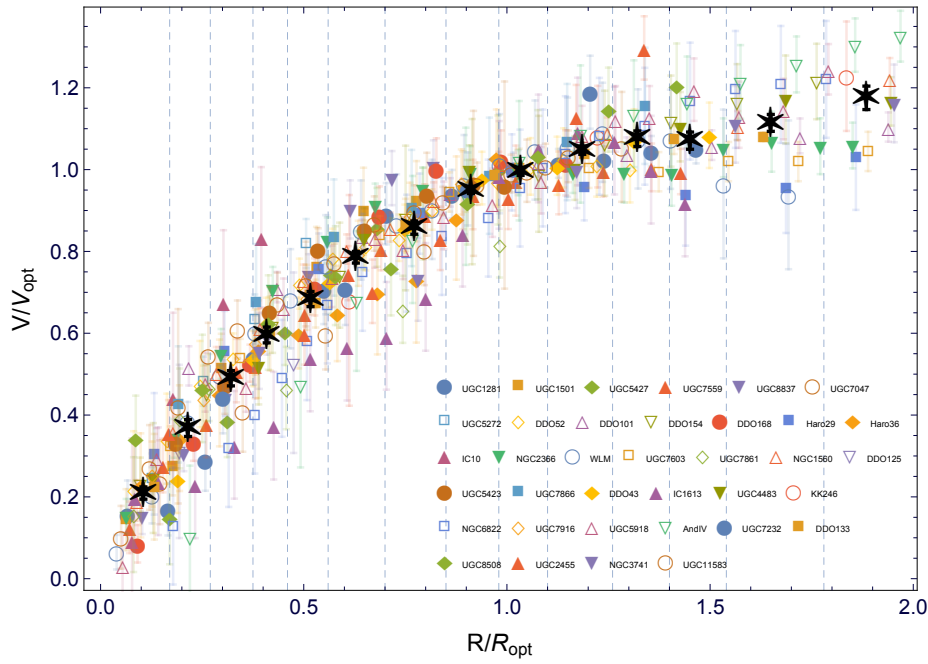


Fig. 11 Individual RCs normalized to R_{opt} and V_{opt} . Also shown the coadded curve (*black stars*). The bins are indicated by vertical dashed grey lines.

radius, this occurs, for each galaxy, at a very different pace. This behavior is related to the very large scatter of the R_{opt} vs L_K relationship, evident in Fig. (1) and absent in normal spirals. In fact, let us double normalize the 36 $V(r)$ to their R_{opt} and V_{opt} values and then derive the quantity $v(x) \equiv V(r/R_{opt})/V(R_{opt})$. This quantity has a unique profile for all objects (see Fig 10, *bottom*): the double normalization of the RC has eliminated most of their original diversity. All the RCs of the Sample are then placed in a same luminosity bin (see Fig (11)).

We coadd the double normalized 350 velocity data by setting 14 radial bins centred at r_i ($i = 1, 14$). Every bin has a number of data from a maximum of 68 to a minimum of 14. Then, by averaging the data in each radial bin i we derive v_i , the coadded (double normalized) rotation velocity at r_i : $v_i = V(r_i/R_{opt})/V(R_{opt})$, their r.m.s. σ_i and residuals $dv_{ij} = v_{ij} - v_i$. The two latter quantities result always very small ([18]) as required by the URC paradigm. The individual RC's (*different colors*) and the coadded one (*big stars*) are shown in Fig(11).

The **dd** luminosity range is as large as that of spirals (PSS). However, differently from them, their rotation curves show all the same (two-normalized) profile and precisely that of the coadded rotation curve of the least luminous normal spirals, with $M_I \simeq -18.5$ (see [31,18]). From this magnitude down, in all disk systems, the RC profile becomes a solid-body like: $V(r) \propto r$ and the stellar disc contribution disappears from the kinematics.

We build the coadded *fiducial* rotation curve: first, for simplicity, we rescale the double normalized velocities v_i to the average values of the sample: $\langle V_{opt} \rangle$ and $\langle R_{opt} \rangle$, 40.0 km/s and 2.5 kpc. So, $\langle V_i \rangle = v_i \langle V_{opt} \rangle$ and $\langle R_i \rangle = r_i \langle R_{opt} \rangle$. The

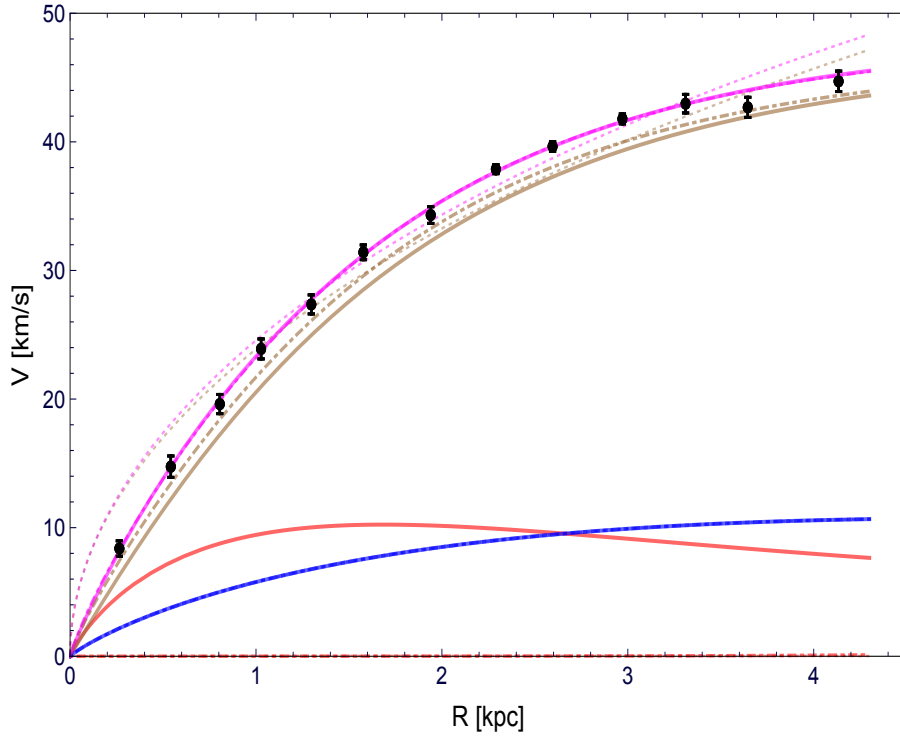


Fig. 12 The coadded **dd** RC (*filled circles*) fitted by the URC (*pink solid line*) and by NFW (*pink dashed line*) profiles. Also shown the relative contributions by stellar disc (*red line*), HI disc (*blue line*) and dark halo (*brown line*)

coadded *fiducial dd* RC extends out to $1.9 \langle R_{opt} \rangle$ and it has uncertainties of $\sim 5\%$ (see Fig(11)).

The URC, in the present case: $V_{URC}(x, \langle V_{opt} \rangle)$, is the *halo + disks velocity model* that fits the fiducial **dd** coadded RC, shown in Fig. (11) as big stars and in Fig (12) as filled circles with errorbars. It consists into the sum, in quadrature, of three terms: V_{URCd} , V_{URCHI} , V_{URCh} that describe the stellar disc, the HI disc and the dark halo contributions. The **dd** galaxies in the sample have all Freeman surface density profile [14]: that leads to the velocity term given in Eq.(5). For the HI component we have: $V_{URCHI}^2(r) = 1/9 V_d^2(x/3) M_{HI}/M_D$ [44]. Moreover: $\langle M_{HI} \rangle = 1.7 \times 10^8 M_\odot$ (see [46]).

For the DM halo we use alternatively the Burkert and the NFW profiles introduced in the previous sections. The URC model fits very successfully the fiducial RC (see Fig.(12)) $\chi_{reduced}^2 < 1$ and the best fit values of the parameters are:

$$\log\langle\rho_0\rangle = 7.55 \pm 0.04 \quad \langle r_0 \rangle = 2.3 \pm 0.13 \quad \log\langle M_D \rangle = 7.7 \pm 0.15$$

where (ρ_0, r_0, M_D) are in units of $(M_\odot/kpc^3, kpc, M_\odot)$. The resulting virial mass is $\langle M_{vir} \rangle = (1.38 \pm 0.05) \times 10^{10} M_\odot$.

Instead, the NFW profile fails to reproduce the coadded RC (see dashed lines in Fig (12)), $\chi_{reduced}^2 \approx 12$ and the values of the best-fit parameters are

$$\log\langle M_{vir} \rangle = 11.7 \pm 0.9 \quad \langle c \rangle = 4.7 \pm 3.2; \quad \log\langle M_D \rangle = 2.5_{-2.5}^{+?}$$

where the two masses, in units of $\log M_\odot$, are totally unrealistic.

By connecting the best fitting values of the core radii with the corresponding stellar disk length-scales we have that also **dd** stay on the line:

$$\log r_0 = 0.47 + 1.38 \log R_D \quad (15)$$

found in Spirals ([38]).

Since: *a)* the double normalized coadded RC is very good fitted by the **dd** URC and *b)* given the strong correlation of Eq.(14), it is possible to obtain from the double normalized URC $V(r/\langle R_{opt} \rangle)/\langle V_{opt} \rangle$ the structural parameters of each galaxy of the sample.. The procedure is the following (see also [18]): in each galaxy, we have, for both disk components:

$$\frac{M_{D,HI}}{V_{opt}^2 R_{opt}} = \frac{\langle M_{D,HI} \rangle}{\langle V_{opt}^2 \rangle \langle R_{opt} \rangle}.$$

We also assume that average value $\frac{\langle V_D^2(R_{opt}) \rangle}{\langle V_{HI}^2(R_{opt}) \rangle} \simeq 1.1$ holds in all the objects. Therefore, for each galaxy of the sample we have that: e.g. the DM mass inside R_{opt} takes the form:

$$M_{DM}(R_{opt}) = (1 - \alpha) V_{opt}^2 R_{opt} G^{-1}$$

, where M_{DM} is the DM mass inside the optical radius R_{opt} and α is the fraction with which the baryonic matter contributes to the total circular velocity. Then:

$$\alpha = \frac{\langle V_{HI}^2(R_{opt}) \rangle + \langle V_D^2(R_{opt}) \rangle}{\langle V_{tot}^2(R_{opt}) \rangle} = 0.12. \quad (16)$$

i.e. α is constant over the objects of the sample. Then, for each galaxy, by inserting in the above equations its values for R_{opt} , V_{opt} , we obtain its dark and the luminous structural parameters. Thus, we realize that **dd** live in haloes with masses below $5 \times 10^{10} M_\odot$ and above $4 \times 10^8 M_\odot$.

Also in **dd** the central surface density of the DM haloes proportional to the product $\rho_0 r_0$, is found to be constant (see Fig. (13)), specifically, within 0.25 dex the value found in spirals [8]. Noticeably, for both galactic systems there is not a satisfactory physical explanation for these two observational evidences.

4.1 A further galaxy structural parameter: the compactness

In **dd** galaxies, differently from Spirals, the disk length scale R_D is not directly related with the virial mass M_{vir} , see Fig(14). This prevent us from straightforwardly converting, as we do in Spirals, the URC expressed in normalized radius x to that expressed in the physical radius r (in fact, in spirals: $r = x R_D(M_{vir})$). We can obtain this conversion, by introducing, for each galaxy of our Sample, a new observational quantity, related to the distribution of stellar disk: the compactness

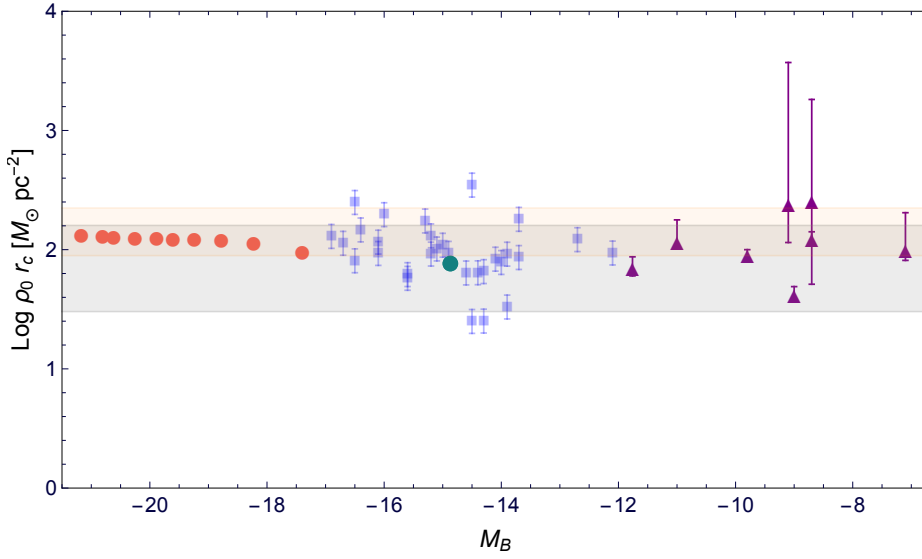


Fig. 13 $\rho_0 r_c$ in units of $M_\odot pc^{-2}$ as a function of magnitude for galaxies of different Hubble Types. Data come from: [38] URC of spirals (*red circles*); the scaling relation from [8] (*orange shadowed area*); the Milky Way dSphs (purple triangles) [35]; **dd** (blue squares-this work), the empirical relation: $\rho_0 r_c = 75_{-45}^{+85} M_\odot pc^{-2}$ from [3] (*grey shadowed area*).

C_* , defined as the ratio between the value of R_D derived from the disk mass M_D through the regression $\log R_D$ vs $\log M_D$ found for the whole sample, and the value R_D directly measured from the photometry. For the Sample of **dd** under study we find: $\log R_D = -3.64 + 0.46 \log M_D$. Then,

$$\log C_* = -3.64 + 0.46 \log M_D - \log R_D \quad (17)$$

$\log C_*$ defines for the Galaxies of a Sample the differences in the sizes of their stellar discs when all objects are reduced to a same stellar mass. We find, with a negligible scatter:

$$\log (R_D/kpc) = -4 + 0.38 \log (M_{vir}/M_\odot) - 0.94 \log C_*. \quad (18)$$

see Fig(14) This result brings two important consequences: i) in **dd** the URC expressed in physical units has two controlling parameters: the luminosity and the compactness. ii) it is remarkable and presently unexplained that two secondary properties of the stellar discs of Galaxies, both belonging to the Luminous World, enter to set a tight relationship with the dark halo mass the most important tag of the dark world of spirals.

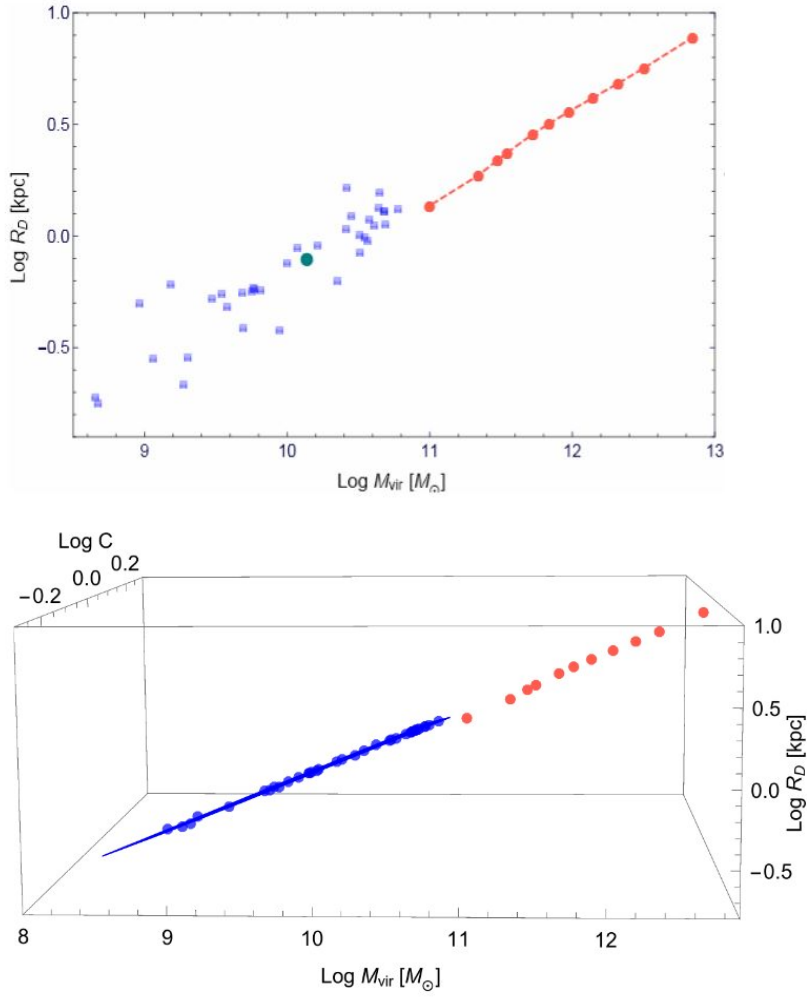


Fig. 14 The the disc length scale versus the halo virial mass. Red circles represent the (967) spirals, blue squares represent the **dd** (*top panel*). The relationship, after involving the compactness $\log C_*$ in the **dd** (*bottom panel*)

5 The McGaugh et al 2016 two-acceleration relationship: a challenge for Dark Matter?

According to recent results ([22]) fueled by the kinematical and photometric data of 153 spirals, the total radial acceleration of the latter,

$$g \equiv V^2/r \quad (19)$$

where $V(r)$ is the circular velocity, shows an anomaly. It correlates, at any radius and in any object, with its component generated *only* from the baryonic matter

$$g_b \equiv V_b^2/r \quad (20)$$

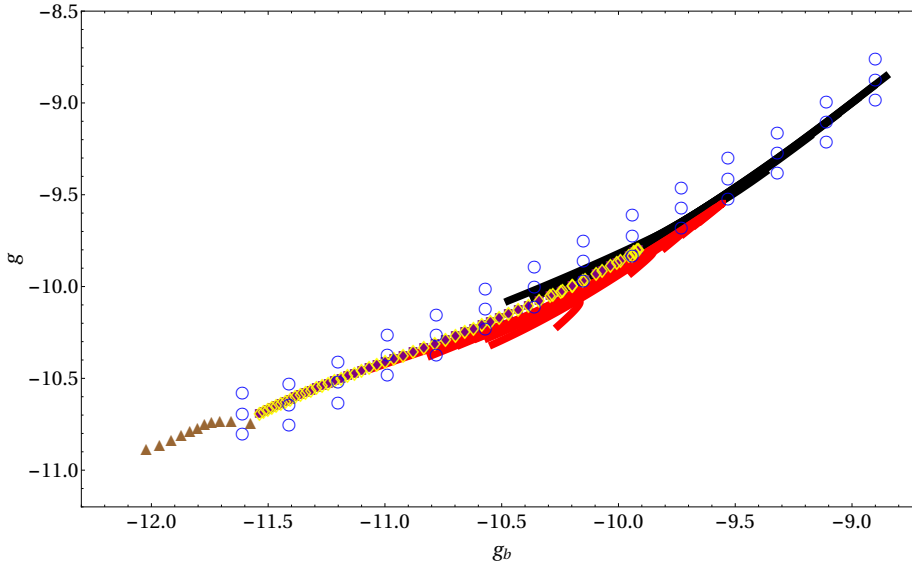


Fig. 15 The region of the McGaugh et al. 2016 relationship in the g - g_b plane including its 1 - σ uncertainty (blue circles). Also shown the relationships found by [39] (red/black lines, blue squares/yellow diamonds/brown triangles points). Accelerations are in units of $\text{Log } m/s^2$

where $V_b(r)$ is the baryonic contribution to $V(r)$ see Fig (15). The baryonic matter, therefore, seems to command the total matter on how to move. This may indicate a very exotic nature for the Dark particle, or the need for an alternative to the DM paradigm or even, a falsification of the Galilean Inertia Law [23]. In any case, is it that true that: "the (above) relationship appears to be a law of Nature, a sort of Kepler's law for rotating galaxies" (McGaugh et al. (2016))?

In fact, all this must be gauged to the phenomenology of the mass distribution of Spirals within the dark matter + Newtonian Gravity paradigm, (see previous sections).

Let us start with

$$g(r) = g_h(r) + g_b(r) \quad (21)$$

$g(r)$ is the total radial acceleration, while $g_h(r)$, $g_b(r)$ are its components generated by the DM halo and by the baryonic matter, respectively. In detail, at any radius r , we have:

$$g_b = (V_d^2 + V_{bu}^2 + V_{HI}^2)/r = g - g_h, \quad g_h = V_h^2/r \quad (22)$$

where all above quantities are function of galactocentric radius r

In detail, McGaugh et al. (2016) have investigated a sample of 153 galaxies across a large range of scales in luminosity and Hubble Types and with high quality rotation curves $V(r)$. For each object, they derived, at any radius with the RC measurement, the radial acceleration $g(r)$ out to outer galactic radii and then compared it with the corresponding value of $g_b(r)$ and the acceleration generated by all the luminous matter of the galaxy. In order to derive the latter accelerations, they used the galaxy surface brightnesses and assumed reasonable values for the mass/light ratios of the disk and bulge surface/volume densities. Then they

inserted them into the relative Poisson equation. Noticeably, this procedure takes in consideration also stellar disks non perfectly Freeman-like.

The relationship they found is displayed as blue circles in Figure (15), extends in g_b for about 3 orders of magnitudes, with a r.m.s (and a systematics) of 0.11 dex ([22]). Quantitatively, the relation reads as:

$$g(r) = g_b(r)/(1 - \text{Exp}[-(g_b(r)/a_0)^{0.5}]) \quad (23)$$

with $a_0 = 1.2 \times 10^{-10} \text{ m/s}^2$ [22]. It implies that the baryonic component of the radial acceleration predicts the latter within a $1-\sigma$ uncertainty of $\pm 13\%$ (see [22]). At low g, g_b accelerations, the relation in Eq.(23) and Fig (15) is clearly very different from that expected in the Newtonian no Dark Matter framework: $g(r) = g_b(r)$, where the centrifugal acceleration balances the gravitational acceleration arising from the distribution of all the baryons in the galaxy.

[39] has independently confirmed and statistically extended the results of [22] by applying three different methods, that *assume* the presence of DM halos as the origin of no-keplerian features in the accelerations, to 100000 accelerations measurements from about 1200 spirals (see Fig (13)).

5.1 The origin of the g vs g_b relationship in Spiral Galaxies

The latter results conciliate the McGaugh et al relationship and the Dark Matter paradigm. However the decisive step is to interpret such relationship. For this purpose, we use $V_G(x)$, a model for the circular velocity of Spirals that hereafter will be called "General". At any x , we set

$$V_G^2(x) = V_{Gh}^2(x) + V_{Gd}^2(x) + V_{GHI}^2(x) \quad (24)$$

where we adopt the Freeman velocity profile of Eq. (5) for the stellar disk component and Eq. (17) for the HI disk component. For the dark halo component, we assume:

$$V_{Gh}^2(x) = 8.5 \cdot 10^5 M_D/R_D B x^{d+1}/(\gamma^2 + x^2) (M_D/(10^{11} M_\odot))^a (km/s)^2 \quad (25)$$

with M_D in M_\odot and R_D in kpc. In detail, B is proportional to the fractional content of dark matter at R_{opt} , a specifies the dependence of the latter quantity on the disk mass, γ measures the size of DM halo core in units of R_{opt} and d indicates how compact is the distribution of dark matter with respect to that of the stars. The disk mass M_D is the running variable, $10^9 M_\odot \leq M_D \leq 4 \times 10^{11} M_\odot$, that describes the entire family of spirals. The General halo velocity model in Eq. (24) is very flexible, it can represent very different DM density profiles, including the NFW and the Burkert ones. We have:

$$g_G(x) = V_G^2(x, M_D)/(x R_{opt}) \quad (26)$$

$$g_{bG}(x) = (V_G^2(x, M_D) - V_{Gh}^2(x, M_D) - V_{GHI}^2(x, M_D))/(x R_{opt}) \quad (27)$$

We use the General model and the relationship in Eq. (4) to fit the data of the McGaugh et al. (2016) relationship (see Fig (16)). The fit is excellent and the best fit values are

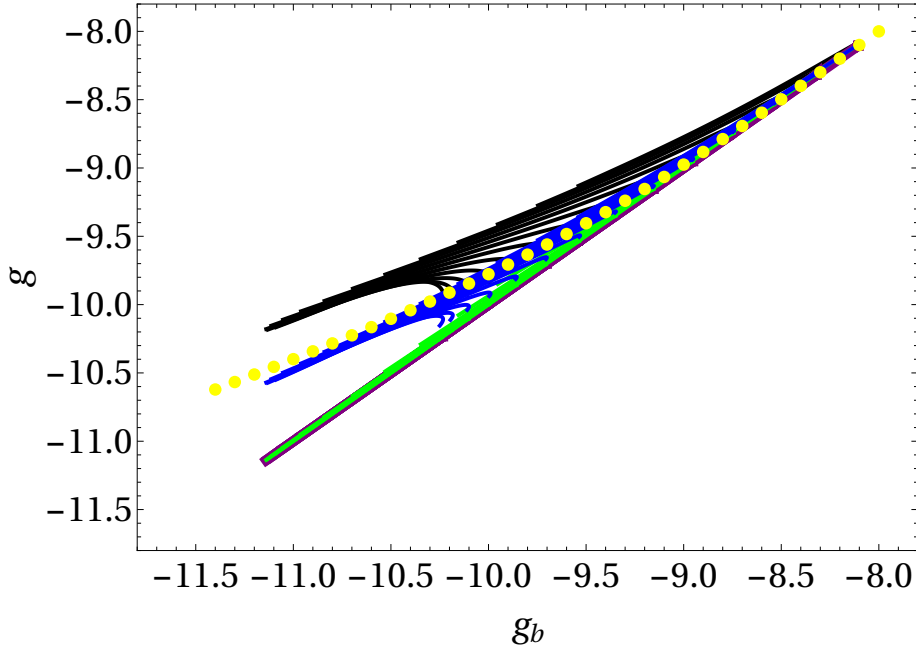


Fig. 16 The McGaugh et al. (2016) relationship (yellow points) best fitted by the General model (blue thick lines). Also shown the latter in the cases of -no dark matter (red lines), -compact dark matter (purple lines) - all dominating dark matter (black lines) and -fraction of DM at R_{opt} increasing with luminosity (green lines).

$$\gamma = 1, a = -1/2, d = 2, B = 0.1$$

(see Fig(16)). The fitting uncertainties of these parameters are about 15%. Let us now determine the cases in which the accelerations from the General model *fail* to recover the McGaugh et al. (2016) relationship. The parameter γ plays little role in the agreement between these two relationships: we can take $0.4 < \alpha < \infty$ without breaking it. The McGaugh, 2016 relationship is blind to the inner distribution of dark matter. Instead, for values $B \simeq 0$ (no dark matter) or $B > 0.3$ which corresponds to an amount of DM > 3 times the best fit value, the General model fails to reproduce McGaugh et al. (2016) relationship (see Fig (15)). Similarly, the agreement between the relationships continues for values of d different from the best fit value of 2, but, for $d < -2/3$, i.e. for a DM halo more compact than the luminous matter, the agreement breaks down. Finally, the agreement breaks down if the quantity $c > 0$ (see Fig(16)) that indicates that, at any x , there must be a larger fraction of DM in the higher luminosity objects.

Therefore, the McGaugh et al. (2016) relationship exists because and only because, in spirals, dark and luminous matter are distributed in the following way:

- *i*) in every object the luminous matter is more concentrated than the dark matter: the quantity $g_h(r)/g_b(r)$ increases with radius r

- *ii*) at any fixed radius x , the lower is the luminosity of the object, the larger is the fraction of dark matter: the quantity $g_h(x, M_I)/g_b(x, M_I)$ increases with decreasing galaxy luminosity.

It is easy to show that *i*) and *ii*) lead to the above $g(g_b)$ relationship. They are known long since to arise from well known astrophysics ([30], [1]). Evidence *i*) originates from the fact that the dark particles are virtually collisionless with respect to the baryonic particles (e.g. [41, 45], [6]). Evidence *ii*) is related to the fact that the smaller the gravitational potential well is, the more efficiently the energy injected into the interstellar space by Supernovae explosions can remove the neutral hydrogen of the galaxies, preventing it to be turned into stars. (e.g. [6]) It is worth to mention that *i*), and *ii*) are found in the Hydro N-Body simulations performed in Λ CDM scenario e.g. [41]

The paradigm of halo dark matter around spirals is therefore totally compatible with the McGaugh et al. (2016) relationship, that, in turn, acquires a physical explanation. The McGaugh relationship does not challenge the Λ CDM scenario. In fact, as a confirm, a very similar relationships directly emerges in a set of well-resolved galaxies in the EAGLE suite of Λ CDM hydrodynamic simulations [21].

6 Conclusions

Thirty years of investigations have secured the evidence of a dark component around the disk of galaxies of any luminosity. The rotation curves of disk systems, excellent tracers of their gravitational fields, are described by an universal profile $V_{URC}(r/R_{opt}, M_I)$ which is incompatible with their distribution of star and gas. Noticeably, the URC, although amply dominated by the Dark Matter component, is a function of *a*) the radius in units of disk length-scale $R_D = 1/3.2 R_{opt}$, *b*) the magnitude M_I , and *c*) the stellar concentration C , all quantities of the luminous component. This is extremely remarkable and it could indicate a non-standard nature of the dark matter.

Furthermore, by modelling the URC with standard disk + halo components, we find that the three parameters of the velocity model: the disk mass M_D , the DM core radius r_0 and the central density ρ_0 are all interrelated to each other and to the galaxy luminosity. This result, in connection with the cored density profiles routinely found in spirals, seems to be at variance with the paradigm of collisionless dark matter and to indicate us that the distribution of matter in galaxies might be a portal for new physics.

The main alternative (not discussed in the work) to this change of paradigm is to upgrade the baryonic components to a crucial role during the period of the formation of spiral's disks (e.g. [7, 43]). In this scenario it is proposed that stars, when go supernovae, can transfer their original nuclear energy to the kinetical energy of the DM particles. This process, could modify a cusped DM halo density distribution into one with a flat inner core and, in addition, it could create the ensemble of the relationships among the halo and disk structural parameters, found in Spirals.

The URC plays also a decisive role in the investigation on the recent claim, raised by McGaugh et al. 2016, of a further challenge to the paradigm of Newtonian DM halos based on the finding of a tight correlation, at any galactic radius of any

spiral, between the radial acceleration $g(r)$ and its baryonic component $g_b(r)$. The URC, in fact, confirms the existence of such relation in normal Spirals, but, at the same time, shows that this relation exists also within the standard DM halo paradigm and it has simple physical explanations.

Acknowledgements I would like to thank the Specola Vaticana and the Organizers of the Workshop “Black Holes, Gravitational Waves and Spacetime Singularities” where this paper has been conceived and Gabriele Gionti for useful discussions.

References

1. Ashman, K. M. 1992, PASP, 104, 1109
2. Bosma, A. 1981, AJ, 86, 1825
3. Burkert A., 2015, ApJ, 808, 158
4. de Blok, W.J.G., Bosma, A., 2002, A&A, 385, 816
5. de Blok W.J. G 2010 AdAst, 2010,5D
6. Dekel A., Silk J., 1986, ApJ, 303, 39
7. Di Cintio A., Brook C. B., Macciò et al., 2014, Mon. Not. R. Astron. Soc., , 437, 415
8. Donato F., Gentile, G., Salucci, P., et al., 2009, Mon. Not. R. Astron. Soc., 397, 1169
9. Donato, F., Gentile, G., Salucci, P., 2004, Mon. Not. R. Astron. Soc., 353, L17
10. Dutton A. A., et al., 2014, Mon. Not. R. Astron. Soc., 61.2658 461, 2658 see
11. El-Badry K., Wetzel A., Geha M., et al. 2016, ApJ, 820, 131
12. Evoli, C. Salucci, P. Lapi, A., Danese, L. 2011, ApJ, 743,45
13. Fattahi, A; Navarro, J F.; Sawala, T., Frenk, et al 2016, arXiv160706479
14. Freeman, K. C., 1970, ApJ 160, 811
15. Gentile, G., Salucci, P., Klein, et al. 2004, Mon. Not. R. Astron. Soc., 351, 903
16. Gentile, G. Burkert, A. Salucci, P. Klein, U. Walter, F. 2005, ApJ, 634, 145
17. Klypin et al. (2010)
18. Karukes, E. V., & Salucci, P. 2016, 2017, Mon. Not. R. Astron. Soc., 465, 4703
19. Keller, B. W. & Wadsley G.W. arXiv:1610.06183
20. Kormendy, J., Freeman, K. 2004, IAU Symp, Sydney, Astr. Soc. of the Pacific., 220, 377
21. Ludlow et al. Phys. Rev. Lett. 118, 161103 (2017)
22. McGaugh, S, Lelli, F., Schombert, J., Phys. Rev. Lett. 2016, 117, 201101
23. Milgrom, M arXiv:1609.06642
24. Moore, B. 1994, Nature 370, 629.
25. Navarro J. et al. arXiv:1612.06329
26. Navarro, J. F., Frenk, C. S., White, S. D. M. 1996, Astrophys. J., 462, 563 (NFW).
27. Oman K. A., et al., 2015, 2015, MN, 452, 3650
28. Persic, M., Salucci, P. 1991, Astrophys. J. 368, 60.
29. Persic, M., Salucci, P. 1995, Astroph. J. Suppl. 99, 501.
30. Persic, M., & Salucci, P. 1988, Mon. Not. R. Astron. Soc., 234, 131
31. Persic, M., Salucci, P., Stel, F., 1996, Mon. Not. R. Astron. Soc., 281, 27
32. Rubin, V.C., Ford, W.K., Thonnard, N. 1980, Astrophys. J., 238, 471.
33. Rubin, V. C., Ford, W. K., Jr., Thonnard, N., and Burstein, D. 1982, ApJ, 261, 439
34. Salucci, P. 2001, Mon. Not. Roy. Astron. Soc., 320, 1.
35. Salucci P., 2012 MN, 420, 2034
36. Salucci, P., De Laurentis, M., 2013, Proceed. of Sci. PoS(DSU 2012)012 (arXiv:1302.2268)
37. Salucci, P., Burkert, A. 2000, ApJ, 5379
38. Salucci, P.; Lapi, A.; Tonini, C.; Gentile, et al 2007, Mon. Not. R. Astron. Soc., 378, 41
39. Salucci P. 2017, arXiv:1612.08857
40. Shankar, F. *et al.* 2006, Astrophys. J., 643, 14.
41. Somerville R.S. & Dave, R. 2015, ARAA, 53, 51
42. Spano, M. et al., 2008, MN, 383, 297
43. Teyssier R., Pontzen A., Dubois Y., Read J. I., 2013, Mon. Not. R. Astron. Soc., 429, 3068
44. Tonini, C.; Lapi, A.; Shankar, F.; Salucci, P. 2006, ApJ, 638, 13
45. Weinberg, S., 2008, Cosmology, OUP, Oxford
46. Yegorova, I.A., Salucci, P. 2007, Mon. Not. R. Astron. Soc., 377, 507.